American Journal of Civil Engineering
2022; 10(5): 191-200
http://www.sciencepublishinggroup.com/j/ajce
doi: 10.11648/j.ajce.20221005.13
ISSN: 2330-8729 (Print); ISSN: 2330-8737 (Online)

Study of Clay Soils, Case of Nomayos-Cameroon: Thermophysical and Chemicomechanical Characterization of Clay Bricks Loaded with 30% Palm Kernel Shell Powder

Hamka Hamka Adolphe Claudel[1, *], Djomi Rolland[1], Mveh Chantal Marguerite[2], Tchotang Theodore[1], Touani Chualeu Parfait[1], Ngohe Ekam Paul Salomon[3]

[1]Civil and Mechanical Engineering Laboratory, National Advanced School of Engineering, University of Yaounde I, Yaounde, Cameroon
[2]Applied Computer Science Laboratory, National Advanced School of Engineering, University of Yaounde I, Yaounde, Cameroon
[3]Energetics Laboratory, National Advanced School of Engineering, University of Yaounde I, Yaounde, Cameroon

Email address:

claudelhamka@yahoo.fr (Hamka Hamka Adolphe Claudel), rdjomi@yahoo.fr (Djomi Rolland), cmmveh@yahoo.fr (Mveh Chantal Marguerite), tchotang@yahoo.fr (Tchotang Theodore), michaeltouani@gmail.com (Touani Chualeu Parfait), pasanek@yahoo.fr (Ngohe Ekam Paul Salomon)

[*]Corresponding author

To cite this article:

Hamka Hamka Adolphe Claudel, Djomi Rolland, Mveh Chantal Marguerite, Tchotang Theodore, Touani Chualeu Parfait, Ngohe Ekam Paul Salomon. Study of Clay Soils, Case of Nomayos-Cameroon: Thermophysical and Chemicomechanical Characterization of Clay Bricks Loaded with 30% Palm Kernel Shell Powder. *American Journal of Civil Engineering*. Vol. 10, No. 5, 2022, pp. 191-200.
doi: 10.11648/j.ajce.20221005.13

Received: September 1, 2022; **Accepted**: September 15, 2022; **Published**: October 11, 2022

Abstract: The work presented in this article consists in demonstrating that the mixture of clay from clay soils and palm nut shell powder is possible for the production of raw clay bricks. For that, we have made characterizations of the mixture of the powder of shells of palm kernel and the clay resulting from the argillaceous grounds of Nomayos which was the subject of a publication. Then, we made the bricks with 0% of load and with 30% of load that we had characterized physically, chemically, thermally and mechanically. The results of the physical characterization allowed us to conclude that the density of the material decreases when it is loaded with 30% of palm kernel shell powder but increases and improves the resistance to bending and compression for the same percentage of load. For the results of the thermal characterization, the ATG, the DSC and the DTG showed: for the clay brick, the presence of free water, Kaolinite, illite and Quartz in important proportion affirming that this clay is of the kaolinite type. For the shells, the presence of free water, cellulose, and lignin; for the mixture with 30% of palm kernel shell powder, the presence of both free water, Kaolinite, illite, Quartz, cellulose, and lignin showing the presence of both clay and shells in the mixture. For the results of the chemical characterization, FTIR showed: for clay, the presence of adsorption bands at 2931 cm^{-1} and 2865 cm^{-1}, absorption peaks at 1554 cm^{-1}, 1494 cm^{-1} and 693 cm^{-1} and a peak near 1307 cm^{-1}. For the shells, the presence of intensity bands at 2924.39 cm^{-1}, average intensity of the fine band between 1509.08 cm^{-1} and 1606.26 cm^{-1}, intensity peaks between 1372.10 cm^{-1} and 1317.91 then 1239.65-1030.05 cm^{-1}. For the clay-shell mixture, the presence of adsorption bands at 2931 cm^{-1} and 2865 cm^{-1} corresponding to asymmetric and symmetric elongation vibrations of the $-CH_2$ groups showing the presence of the clay silane. The peaks of intensity between 1239.65 and 1030.05 cm^{-1} can be attributed to the -C-O groups of alcohols, Esther, ether, amorphous silica or -C-O bonds of celluloses and lignins showing the presence of the shells in the mixture.

Keywords: Clay Bricks, ATG, IRTF, Compressive Strength, Flexural Strength

1. Introduction

For thousands of years, earthen constructions have been in great demand. The housing crisis is currently forcing developing countries to ask researchers to focus on the revaluation of local materials, biodegradable and

environmentally friendly. It is estimated that 30% of the houses in the world are built from earth [1]. From the earth material is extracted clay, which is one of the materials containing natural minerals most abundant on earth. This while for the manufacture of bricks, clay must have certain properties and characteristics that allow them to be easily shaped and molded when mixed or reinforced with fibers or vegetable fillers. Clay bricks are one of the oldest building materials. The oldest mud bricks can be found in the ruins of many ancient civilizations such as Egypt and the Indus Valley [2]. Despite all this, mud brick constructions have a very limited life span [3]. This may be due to a lack of strength, systematic cracking due to shrinkage and the problem of sensitivity to water [4, 5]. Several studies have demonstrated the importance of reinforcement or stabilizer in brick constructions following the example of Kazmi et al, who reinforced clay bricks with sugarcane bagasse ash (SBA) and rice husk ash (RHA) [6]: They demonstrated in their work that this reinforcement gives the brick good lightness, durability and mechanical strength. Similarly, Munir et al reinforced clay bricks with waste marble powder [7]. Their study revealed that the replacement led to lighter bricks with reduced linear shrinkage and mechanical strength and finally Javed et al demonstrated that reinforcing bricks with lime and bentonite decreases the weight of the brick and increases the mechanical strength and reduces the thermal conductivity [8]. From the above, we can formulate the hypothesis that the reinforcements such as fibers, particles, influence the characteristics (mechanical; chemical, thermal....) of the earth bricks. Observations show that the degradation of earth bricks in association with these vegetable fibers is faster [9]. Given the importance and rigor in the field of building construction, this problem becomes a danger to the lives of people (cracks, collapses...). Research has come to the conclusion that solutions must be found to solve this problem and for some years now, palm kernel shells have been the subject of several research studies, such as Epesse and al. for their use as fuel [10]; Ernesto de la tore and al.; Hidayu et al. for the production of activated carbon [11, 12] and Djomi and al. as a reinforcement for the production of PVC [13], and these studies have yielded favorable results. In view of these research results, what could be the behavior of clay bricks reinforced with palm kernel shell powder?

2. Materials and Experimental Methods

2.1. Materials

2.1.1. For Physical Properties

Digital scale at 1/100th; A digital caliper at 1/50th; An automatic mixer of table provided with an agitator of mark Maurice PERRIER and Co, 20 rue Marie Debos 92120. MONTROUGE (France), Type 32, No 651 of the laboratory of geotechnics of the national polytechnic school of Yaoundé; a shock table provided with a mould of dimension 160x40x40.

2.1.2. For Mechanical Properties

A three-point bending and electrohydraulic compression testing machine Impact Test Equipment Limited, 250 KN from the organic chemistry laboratory of the University of Yaoundé 1 [14].

Figure 1. *Electrohydraulic three-point compression and bending testing machine Impact Test Equipment Limited.*

2.1.3. For Thermal Properties

A LENSEIS instrument with an alumina oxide crucible and a capacity of 150 mg. The heating rate is 10°/min. The gas used is oxygen and nitrogen [13].

2.1.4. For Chemical Properties

An Alpha spectrometer from Bruker analyzed by the ATR (Attenuated Total Reflection) technique on a diamond crystal. The resolution during the collection of the spectra is fixed at 4 cm^{-1}, from the laboratory of physical and analytical chemistry of the University of Yaoundé 1 [15].

Figure 2. *Process of obtaining the specimens.*

2.2. Experimental Methodology

2.2.1. Elaboration of the Specimens

From Figure 2a, we observe the process of mixing clay from clay soil and palm kernel shell powder loaded to 30%. According to the work of Huisken and al in 2022, the Laws of mixtures are calculated according to the relationship (1) and applied in this work [16].

$$\begin{cases} M_f = \frac{\rho_f}{\rho_c} V_f \Rightarrow M_f = \frac{\rho_f}{\rho_f . V_f + \rho_m (1 - V_f)} V_f \\ M_m = \frac{\rho_m}{\rho_c} V_m \Rightarrow M_m = \frac{\rho_m}{\rho_f . V_f + \rho_m (1 - V_f)} V_m \end{cases} \quad (1)$$

From Figure 2b, we observe the mixing process between the clay and the palm kernel shell powder loaded to 30%, this to get as close as possible to the model of a homogeneous and isotropic material. The mixing is done with an automatic mixer of the laboratory of geotechnics and materials of the National Polytechnic School of Yaoundé (ENSPY).

From Figure 2c, we observe the molding process of the mixture of clay and palm nut shell powder loaded at 30%. The mixture is filled, then packed in the molds (160x40x40 mm) so that the future specimens have the same thickness. The compression of the specimens is done at 10bars, using a shock table that makes 60 shocks / minutes at room temperature. This pressure guarantees a good cohesion of the material.

From the figure 2d, we obtain the specimens. These specimens are stored in the shade and out of the sun, to avoid a too strong and brutal shrinkage, cause of many cracks. We have chosen a corner of the laboratory for this purpose.

2.2.2. Physical Properties: Apparent Density

The methodology is as follows:

1) Take the dimensions of each test piece using a digital caliper at 1/50th;
2) Measure the mass of the different test specimens using a digital balance to 1/100th;
3) Determine the respective volume of the specimens from the measured dimensions ($V = L\ x\ l\ x\ e$);
4) Determine the bulk density of each composite material ($\rho = {}^{m}/_{v}$).

$$V = Lxlxe \quad (2)$$

$$\rho = \frac{m}{V} \quad (3)$$

L: Length of the test piece;
l: width of the specimen;
e: thickness of the specimen;
m: mass of the specimen;
V: volume of the specimen;
ρ: Density of the test specimen.

2.2.3. Mechanical Properties

(i). Bending Test

The methodology is as follows:

1) The specimen of size 160x40x40 is previously positioned on the two supports of the machine;
2) The load is applied gradually, at equal distance from the supports at regular time intervals (time necessary for the deflection to stabilize) between the platens of the electrohydraulic press Impact Test Equipment Limited, 250 KN until the material breaks; the distance between supports (L) is 80 mm in accordance with the BSI 2782 standard that our specimens comply with. The load and displacement data are collected as they are entered and then processed using the Excel application to plot the force/displacement and resistance/time curves. This test will give us the results of Young's modulus (E) and flexural strength (Rf).
3) The ambient temperature of the test room is between [22°C; 32°C]. The sink rate of the plate was set to 0.1 MPa/s. For each formulation, the strength obtained is the average of the tests performed on three specimens. This measurement was carried out in the Laboratory of Physical and Analytical Chemistry of the University of Yaoundé I.

(ii). Compression Test

The methodology is as follows:

1) The specimen of size 40x40x40 is previously positioned on the two supports of the machine;
2) The test consists of subjecting the specimen to two opposing axial forces located between the platens of the Impact Test Equipment Limited electrohydraulic press, 250 KN (Appendix). The rate of descent of the platen was set at 0.5 MPa/s. For each formulation, the strength obtained is the average of the tests performed on three 40 mm cubic specimens. This test will allow us to have the results of the flexural strength (Rf).

2.2.4. Thermal Properties

The machine is a LENSEIS brand instrument from the organic chemistry laboratory of the University of Yaoundé I with an alumina oxide crucible and a capacity of 150 mg. The heating speed is 10°/min. The gas used is oxygen. The initial mass of the measurements is between 100 mg and 120 mg. The starting temperature of the tests is a function of the ambient temperature (20°C and 35°C). The data acquisition is done by a software incorporated in the machine which allows the automatic recording on a computer. The thermograms and the data of the recordings are given at the end of the analyses. The methodology of the tests is in conformity with the standard and applied in the laboratory. We are provided with the recording data and the ATG and DSC curves. The methodology is the one applied in the work of Djomi and al in 2018 and olembe and al in 2021 [13, 15].

2.2.5. Chemical Properties

An Alpha spectrometer from Bruker analyzed by the ATR (Attenuated Total Reflection) technique on a diamond crystal. The resolution during the collection of the spectra is fixed at 4 cm^{-1}, from the laboratory of physical and analytical chemistry of the University of Yaoundé1. The method used is

by attenuated total reflectance (ATR) whose methodology is standard. The data acquisition is done with the help of a software incorporated in the apparatus which allows the recording and the plot of the spectra automatically on a computer. We are provided with recording data and FTIR spectra [15].

3. Results and Discussion

3.1. Results of Physical Properties: Apparent Density Results

3.1.1. Apparent Density Results for Unfilled Green Bricks

Table 1. *Result of bulk density of unfilled green bricks.*

Apparent density of unfilled mud bricks			
Test tubes	**Epr1**	**Epr2**	**Epr3**
Length (mm)	142.68	142.29	145.63
Width (mm)	35.44	35.13	35.91
Thickness (mm)	35.74	35.63	35.96
Volume (mm^3)	180722.1406	178101.8176	188055.4559
Mass (g)	335.01	333.5	337.05
Density (g/mm^3)	0.00185373	0.001872524	0.00179229
Density (kg/m^3)	1853.729703	1872.524405	1792.290463
Average mass density (kg/m^3)	1839.514857		
Standard deviation	41.96329078		

In view of the various calculations carried out, we note that the experimental density of the various unloaded specimens is between 1792.2904 and 1872.5244 (kg/m^3). This allows us to have an average value of 1839.5148 Kg/m^3.

3.1.2. Bulk Density Results for 30% Filled Green Bricks

Table 2. *Result of bulk density of green bricks loaded at 30%.*

Bulk density of green bricks loaded at 30%.			
Test specimens	**Epr1**	**Epr2**	**Epr3**
Length (mm)	148.54	149.01	147.7
Width (mm)	36.68	36.83	36.69
Thickness (mm)	38.46	37.55	37.25
Volume (mm^3)	209547.2793	206075.8382	201861.9593
Mass (g)	319.05	324.01	314.51
Density (g/mm^3)	0.001522568	0.001572285	0.001558045
Density (kg/m^3)	1522.568086	1572,285246	1558.044919
Average mass density (kg/m^3)	1550.966084		
Standard deviation	25.60334826		

In view of the various calculations made, we note that the experimental density of the various specimens loaded with 30% palm kernel shell powder is between 1522.568086 and 1572.285246 (kg/m^3). This allows us to have an average value of 1550.966084 Kg/m^3.

3.1.3. Influence of Palm Kernel Shell Powder on the Bulk Density of Green Bricks

The observation of the results of this test allows us to note that the palm kernel shell powder loaded at 30% decreases the apparent density. This is explained by the fact that the palm kernel shells have a low density compared to that of the clay. Therefore, they occupy a volume in the mixture that influences its density. These results are close to those obtained by Limami and al in 2020 in his research work [17]. He demonstrated in his work that Lowering the bulk density of the samples produced is in itself an improvement because, a high percentage of polymer additives means a low content of clay, which will allow the production of bricks at low cost, given that polymer additives are abundant and their recycling is highly encouraged. From this analysis, we can therefore justify the results obtained from our clay loaded with palm kernel shell powder.

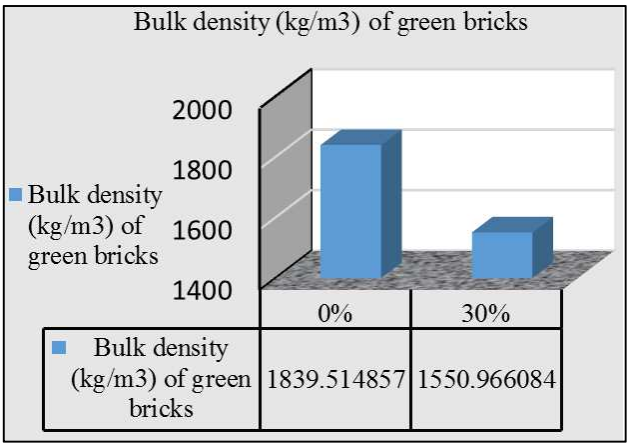

Figure 3. *Influence of palm kernel shell powder on the bulk density of green bricks.*

3.2. Results of Mechanical Properties

3.2.1. Compressive Strength Results (Rc)

(i). Case of Unfilled Green Bricks

Table 3. *Compressive strength results for unfilled green bricks.*

Loading rate	Test specimens	strength (Mpa)	Average strength (Mpa)	Standard deviation
Unfilled raw brick	epr1	1.57	1.4823	0.55075796
	epr2	1.984		
	epr3	0.893		

From the results given by the machine, we can see that the compressive strength of the different unloaded raw specimens is between 0.893 and 1.984 Mpa. This gives us an average compressive strength of 1.4823 Mpa.

(ii). Case of Green Bricks Loaded at 30%

Table 4. *Compressive strength results for green bricks loaded at 30%.*

Loading rate	Test specimens	strength (Mpa))	Average strength (Mpa)	Standard deviation
Raw brick loaded at 30%.	epr1	2.11	2.238	0.23041701
	epr2	2.1		
	epr3	2.504		

In view of the results given by the machine, we note that the compressive strength of the various raw specimens loaded with 30% palm kernel shell powder is between 2.1 and 2.504 Mpa. This allows us to have an average compressive strength of 2.238 Mpa.

Influence of palm kernel shell powder on the compressive strength behavior of green bricks.

The observation of the results of this test allows us to note that, the palm kernel shell powder loaded at 30% improves the compressive strength of our bricks. These results are superior to those obtained by Belaid Fayçal et al. [18], but close to those of Nshimiyimana, P. et al. [19].

3.2.2. Results of the Flexural Strength (Rf): Case of Unfilled Green Bricks

Table 5. *Three-point bending strength results for unloaded green bricks.*

Loading rate	Test specimens	Rf (Mpa)	Average Rf (Mpa)	Standard deviation
Unfilled raw brick	epr1	4.735	4.148666667	0.50801608
	epr2	3.871		
	epr3	3.84		

From the results given by the machine, we see that the flexural strength of the different unloaded specimens is between 3.84 and 4.735 Mpa. This gives us an average flexural strength of 4.1486 Mpa.

Case of green bricks loaded at 30%.

Table 6. *Result of the three-point bending strength of green bricks loaded at 30%.*

Loading rate	Test specimens	Rf (Mpa)	Average Rf (Mpa)	Standard deviation
30% unfilled raw brick	epr1	4.259	4.405	0,226563457
	epr2	4.666		
	epr3	4.29		

In view of the results given by the machine, we note that the flexural strength of the different specimens loaded with 30% of palm kernel shell powder is between 4.259 and 4.666 Mpa. This allows us to have an average flexural strength of 4.405Mpa.

Influence of palm kernel shell powder on the flexural strength behavior of green bricks.

The observation of the results of this test allows us to note that the mixture of palm kernel shell powder loaded at 30% improves the flexural strength of our bricks. These results are superior to those obtained by poullain et al. [20] and also to those of M. Ouedraogo et al. [21] who demonstrated in his work that the adobe reinforced with Kenaf fibers had a higher flexural strength than that of sisal simply because of the biochemical composition of Kenaf which would be better than that of sisal. From this analysis we can therefore explain the reason for the high values of flexural strength of our clay bricks reinforced with palm kernel powder by its rich biochemical composition which would be super ior to that of kenaf and sisal.

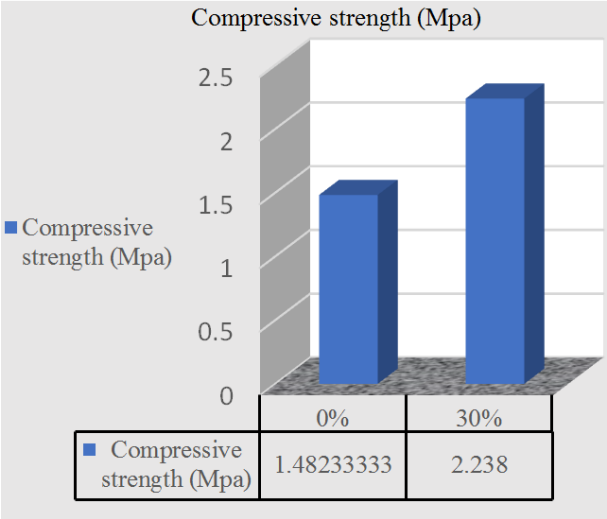

Figure 4. *Influence of palm kernel shell powder on the compressive stress of green bricks.*

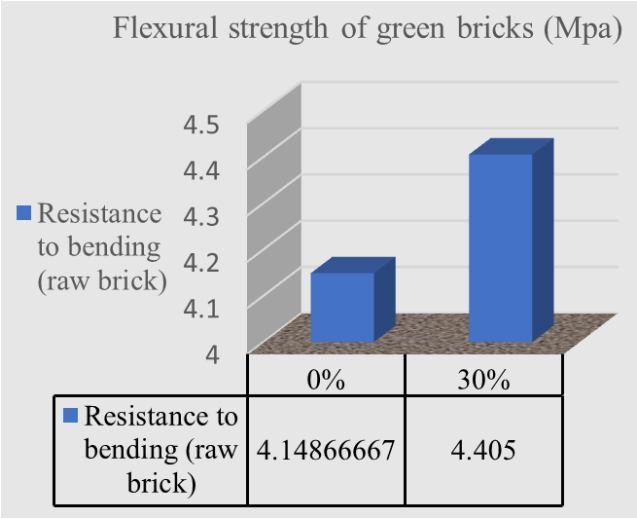

Figre 5. *Influence of palm kernel shell powder on the bending stresses of green bricks.*

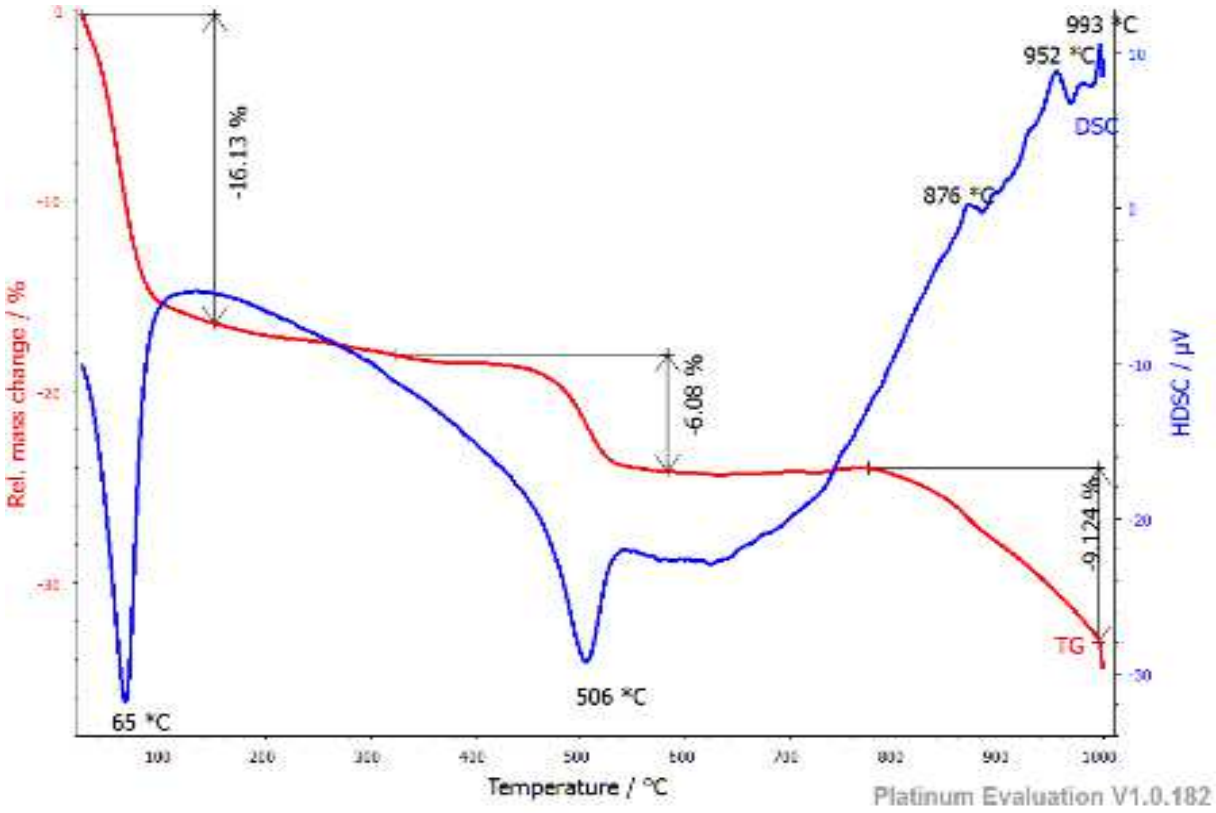

Figure 6. *TG and DSC thermogram of unfilled green clay bricks: TG thermogram, in blue DSC thermogram. And in black the DTG thermogram.*

3.3. Results of the Thermal Properties

3.3.1. Results of Thermogravimetric and Differential Analysis of Unfilled Green Bricks

These analyses allow us to understand the phenomenon of the degradation of the clay material as a function of temperature. The DSC thermogram in blue shows an endothermic heat peak at 65°C. It is the beginning of the dehydration of the clayey material presented by the TG in red color. The DSC shows in addition 4 representative and sensitive peaks of the degradation. These are the peaks at 506°C, 522°C, 876°C and 952°C.

At 65°C, we have an endothermic low which corresponds to the departure of hygroscopic water and zeolitic water from illite; the percentage of loss of mass determined from the ATG curve and is approximately 16.13%;

At 506°C a second endothermic trough marks the departure of the water of constitution of Kaolinite and its

transformation into metakaolinite; here the loss of mass is estimated at 6.08%. This result confirms that of some authors who affirm that the loss of water evolves towards a higher temperature;

At 565°C; we have an endothermic peak which highlights the presence of quartz. This temperature marks the allotropic change of quartz. It passes from quartz α to quartz β. This reaction does not involve any loss of mass [22].

At 952°C, we have an exothermic peak which indicates the formation of mullite from metakaolinite. These thermal analysis results show that our clay sample contains kaolinite, illite and quartz. This confirms that the mineralogical analysis will show kaolinite, illite and quartz [22]. In view of these results, it should be noted that the Nomayos clay is of kaolinic type. The granulometric analysis indicates a fine texture whose essential elements are kaolinite, illite and quartz. Thermal studies also show that this clay can be used for the manufacture of stabilized earthen bricks and fired roof tiles. It can also be used for the production of bricks and other cold stabilized products [22].

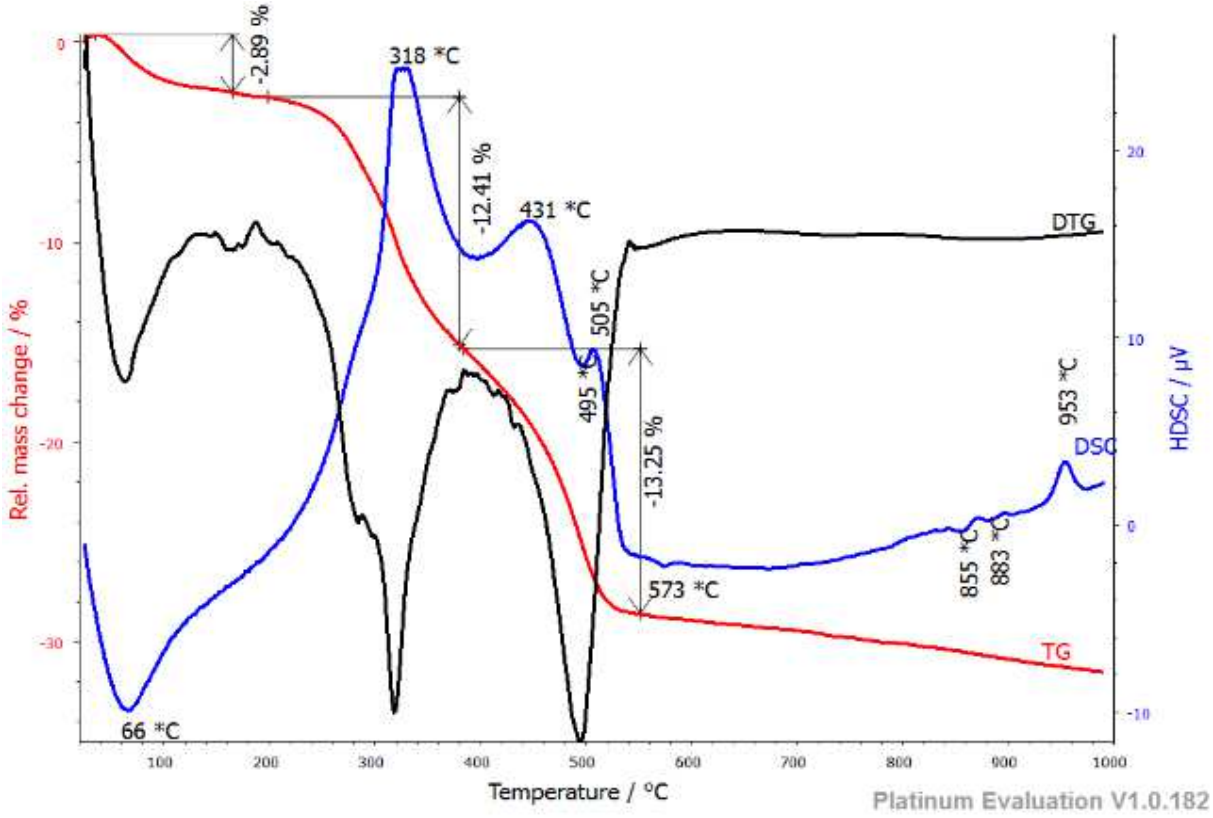

Figure 7. *TG, DSC and DTG thermograms of green clay bricks loaded with 30% shells. In red: TG thermogram, in blue DSC thermogram. And in black the DTG thermogram.*

3.3.2. Results of Thermogravimetric and Differential Analysis of Green Bricks Loaded at 30%

We note on the mixture of DTG curves the presence of hulls and clay.

The endothermic peak observed at 66°C of our mixture of clay and palm kernel powder in Figure 7 corresponding to the departure of water retained on the surface of the clay. The percentage by weight of this loss calculated from the ATG curve is about 2.89%, this rate is mainly due to the percentage in this mixture of the fine fraction of the clay and the fine fraction of the hull powder. These results are similar to those of Osabor et al. [23].

The endothermic peak observed at 318°C is the peak representing the transition between cellulose and lignin [24]. This transition shows at the DSC level the departure of cellulose which represents a loss of 12.41% of the initial mass of the hull powder. Similarly, the peaks from 318°C to 505°C show that the degradation of lignin with a loss of mass of 13.25%. The ash is noticed between 573°C and 600°C where the remaining material does not absorb or release heat [13].

At 505°C a second endothermic peak marks the departure of the water of constitution of Kaolinite and its transformation into metakaolinite;

At 573°C; we have an endothermic peak which highlights the presence of quartz. This temperature marks the allotropic change of quartz. This phase does not lead to a loss of mass.

At 953°C, we have an exothermic peak which indicates the formation of mullite from metakaolinite. At this phase we no longer have the presence of palm kernel shell powder. Here we see the presence of clay constituents such as: kaolinite, illite and quartz. These results of thermal analysis ATG, DTG and DSC show the presence in this mixture of palm kernel shell powder and nomayos clay.

3.4. Results of Chemical Properties

3.4.1. Results of Infrared Oven-Transform Analysis of Unfilled Green Bricks

The oven-transform infrared spectra of the clays show an intense peak at 910.29 cm^{-1} and a band at 523.75cm^{-1} relating to the elongation and torsional vibrations of the Si-O bonds respectively. These results are similar to those of shanmugharaj in his work in 2007 [25] in the same way as Benbayer in his work in 2014 [26], the broad bands at 3651.16cm^{-1} and 1635cm^{-1} are attributable to the elongation and deformation vibrations of -OH and water molecule absorbed in the interfoliar space of clay sheets [27]. The results obtained highlight the presence of two new adsorption bands at 2931 cm^{-1} and 2865 cm^{-1} corresponding to asymmetric and symmetric elongation vibrations of the -CH_2 groups, which shows the presence of silane in the clays. These results obtained on elongation and strain vibrations and then on asymmetric and symmetric elongations of the groups are close to the results of Risite, shanmugharaj and Hongping, in their works on clays in 2015, 2007 and 2004 respectively [28, 25, 29].

The presence of the new absorption peaks at 1554cm^{-1}, 1494cm^{-1}, and 693cm^{-1} corresponding successively to deformation vibrations of -NH_2 and -CH_2 and out of plane deformation of -CH. The peak at 1307 cm^{-1} is attributed to an elongation vibration of C-N. These results obtained in our work are very similar to those obtained by Laibi in his work in 2017 [22].

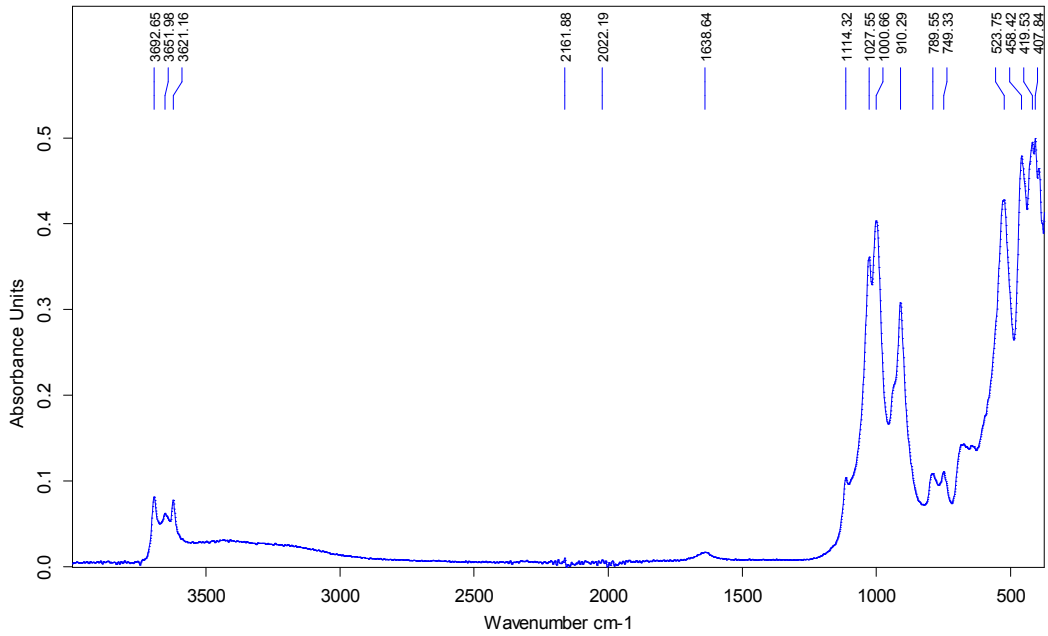

Figure 8. *Fourier transform infrared spectrum of unfilled green bricks.*

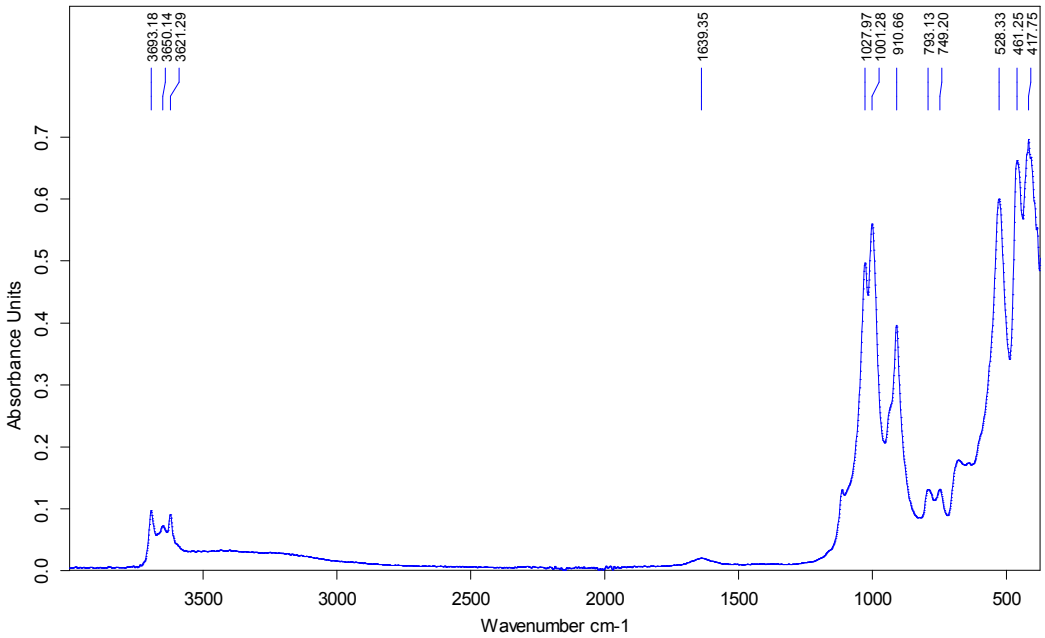

Figure 9. *Fourier transform infrared spectrum of 30% loaded green bricks.*

3.4.2. Results of Infrared Oven-Transformed Analysis of Raw Bricks Loaded at 30%

The oven-transform infrared spectra of the clays show an intense peak at 910.29 cm^{-1} and a band at 523.75cm^{-1} relating to the elongation and torsional vibrations of the Si-O bonds respectively. These results are similar to those of shanmugharaj in his work in 2007 [25] in the same way as Benbayer in his work in 2014 [26], the broad bands at 3651.16cm^{-1} and 1635cm^{-1} are attributable to the elongation and deformation vibrations of -OH and water molecule absorbed in the interfoliar space of the clay sheets [27]. The results obtained highlight the presence of two new adsorption bands at 2931 cm^{-1} and 2865 cm^{-1} corresponding to asymmetric and symmetric elongation vibrations of the $-CH_2$ groups, which shows the presence of silane in the clays. These results obtained on the elongation and strain vibrations and then on the asymmetric and symmetric elongations of the groups are close to the results of Risite, shanmugharaj and Hongping, in their work on clays in 2015, 2007 and 2004 respectively [28, 25, 29].

The presence of the new absorption peaks at 1554cm^{-1}, 1494cm^{-1}, and 693cm^{-1} corresponding successively to deformation vibrations of $-NH_2$ and $-CH_2$ and out of plane deformation of -CH. The peak at 1307 cm^{-1} is attributed to an elongation vibration of C-N. These results obtained in our work are very similar to those obtained by Laibi in his work in 2017 [21] and identical to those of Belver and al in his research work in 2002 [30]. He found that the spectra of his three samples studied merge because they absorb at the same frequency, relatively with the same intensity, which allows him to say, from the mineral point of view that the vibrational bands of the structural hydroxyls (3690cm^{-1} and 3620 cm^{-1}) shows that the acid attack did not destroy or penetrate the crystal structure of kaolinite. In view of this analysis and according to the identical result of Belver et al, we can therefore say that the palm kernel shell powder did not destroy or penetrate the crystalline structure of kaolinite, thus does not influence chemically during mixing.

4. Conclusion

The valorization of local materials for building construction participates in the economic development of a country. Therefore, it requires the mastery of its physical, mechanical, chemical and thermal properties. The results obtained allow to conclude that:

1) The inclusion of 30% hull powder in the clay brick reduces the apparent density, which is favorable for high buildings (several levels).
2) The inclusion of the 30% hull powder in the clay brick considerably improves the mechanical properties, namely the compressive strength and the flexural strength.
3) Chemical analysis indicates that our clay has mostly three (3) oxides namely silica (SiO_2), alumina (Al_2O_3) and iron oxides (Fe_2O_3). and our palm kernel shell powder has the 51% of carbon (C), 8% of hydrogen (H), 32% of oxygen (O), 0.1% of nitrogen (N), 3.9% of water (H_2O) and 5% of ash (K_2CO_3) [10].
4) The thermal analyses allowed us to identify and confirm the minerals contained in the samples of clays, shells and the clay-shell mixture. The results of these thermal analyses will lead us in the future works to the characterization of the fired bricks in order to find a durable, economic and ecological solution for our constructions.

References

[1] Imen, S., & Belouettar, R. (2011). Mechanical behavior of mud bricks reinforced with date palm and straw fibers. INVACO2 International Seminar, Innovation & Valorization in Civil Engineering & Building Materials, (2p-118).

[2] de Chazelles, C. A., & Klein, A. (2003). Transdisciplinary exchanges on raw earth constructions. 1. Shaped, cut or cased earth. Materials and methods of implementation. Doi: https://halshs.archives-ouvertes.fr/halshs-00548079

[3] Chanvillard, G. (1999). Modeling the pullout of wire-drawn steel fibers. Cement and Concrete Research, 29 (7), 1027-1037. Doi: https://doi.org/10.1016/S0008-8846(99)00081-2

[4] Doat, P., Hays, A., Houben, H., Matuk, S., & Vitoux, F. (1979). Building with earth. Alternative and parallel editions. Doi: http://pascal-francis.inist.fr/vibad/index.php?action=getRecordDetail&idt=PASCALBTP8080279395

[5] Guillaud, H., Cope, R., Odul, P., Doat, P., Houben, H., & Verney, P. E. (1986). Scientific and technical approach to the earth material (Doctoral dissertation, CRATerre; CSTB; Ministry of Research and Technology). Doi: https://hal.archives-ouvertes.fr/hal-03162175

[6] Kazmi, S. M., Abbas, S., Saleem, M. A., Munir, M. J., & Khitab, A. (2016). Manufacturing of sustainable clay bricks: Utilization of waste sugarcane bagasse and rice husk ashes. Construction and building materials, 120, 29-41. Doi: https://doi.org/10.1016/j.conbuildmat.2016.05.084

[7] Munir, M. J., Kazmi, S. M. S., Wu, Y. F., Hanif, A., & Khan, M. U. A. (2018). Thermally efficient fired clay bricks incorporating waste marble sludge: An industrial-scale study. Journal of cleaner production, 174, 1122-1135. Doi: https://doi.org/10.1016/j.jclepro.2017.11.060

[8] Javed, U., Khushnood, R. A., Memon, S. A., Jalal, F. E., & Zafar, M. S. (2020). Sustainable incorporation of lime-bentonite clay composite for production of ecofriendly bricks. Journal of Cleaner Production, 263, 121469. Doi: https://doi.org/10.1016/j.jclepro.2020.121469

[9] Hongrattanavichit, I., & Aht-Ong, D. (2020). Nanofibrillation and characterization of sugarcane bagasse agro-waste using water-based steam explosion and high-pressure homogenization. Journal of Cleaner Production, 277, 123471. Doi: https://doi.org/10.1016/j.jclepro.2020.123471

[10] Misse, S. E., Obounou, M., Ohandja, L. A., & Caillat, S. (2013). Use of palm kernel shells as fuel in a scrap metal melting furnace. Journal of Renewable Energies, 16(1), 75-89. Doi: https://doi.org/10.54966/jreen.v16i1.365

[11] De la Torre Chauvin, E. H. (2015). Preparation of activated carbon from oil palm nut shells for gold recovery and cyanide effluent treatment (Doctoral dissertation, UCL- Catholic University of Louvain). http://hdl.handle.net/2078.1/155680

[12] Hidayu, A. R., Sukor, M. Z., Mohammad, N. F., Elham, O. S. J., Azri, N. I., Azhar, M. A. I., & Jalil, M. J. (2019, November). Preparation of activated carbon from palm kernel shell by chemical activation and its application for β-carotene adsorption in crude palm oil. In Journal of Physics: Conference Series (Vol. 1349, No. 1, p. 012103). IOP Publishing. doi: 10.1088/1742-6596/1349/1/012103.

[13] Djomi, R., Meva'a, L. J. R., Nganhou, J., Mbobda, G., Njom, A. E., Bampel, Y. D. M., & Tchinda, J. B. S. (2018). Physicochemical and Thermal Characterization of Dura Palm Kernel Powder as a Load for Polymers: Case of Polyvinyl Chloride. Journal of Materials Science and Chemical Engineering, 6 (6), 1-18. Doi: 10.4236/msce.2018.66001.

[14] Riyap, H. I., Banenzoué, C., Tchakouté, H. K., Nanseu, C. N., & Rüscher, C. H. (2021). A comparative study of the compressive strengths and microstructural properties of geopolymer cements from metakaolin and waste fired brick as aluminosilicate sources. Journal of the Korean Ceramic Society, 58 (2), 236-247. https://doi.org/10.1007/s43207-020-00097-y

[15] Olembe, Y. R., Fokam, C. B., Tchotang, T., Djomi, R., Kenmeugne, B., & François, M. L. M. (2021). Investigation of the Physical, Mechanical and Chemical Properties of the Marrow of Raffia Hookeri. Journal of Natural Fibers, 1-13. https://doi.org/10.1080/15440478.2021.1961337

[16] Huisken, P. W. M., Tchemou, G., Tagne, N. R. S., Ndapeu, D., & Njeugna, E. (2022). Effect of the Addition of Oil Palm Mesocarp Fibers on the Physical and Mechanical Properties of a Polyester Matrix Composite. International Journal of Polymer Science, 2022. https://doi.org/10.1155/2022/3399986

[17] Limami, H., Manssouri, I., Cherkaoui, K., & Khaldoun, A. (2020). Study of the suitability of unfired clay bricks with polymeric HDPE & PET wastes additives as a construction material. Journal of Building Engineering, 27, 100956. https://doi.org/10.1016/j.jobe.2019.100956

[18] Belaid, F., & Chelouah, N. (2020). Study of the influence of Crushed Date Kernels (CDN) additions on the physical-mechanical and thermal characteristics of a compressed raw earth brick (CREB) (Doctoral dissertation, Abderrahmane Mira-Bejaia University). http://hdl.handle.net/123456789/13704

[19] Nshimiyimana, P. (2021). Influence of substitute materials on the microstructure and strength of compressed earth bricks. Academic Journal of Civil Engineering, 39 (1), 144-152. DOI: https://doi.org/10.26168/ajce.39.1.32

[20] Poullain, P., Leklou, N., Laibi, A. B., & Gomina, M. (2019). Properties of Compressed Earth Bricks Made from Traditional Materials from Benin. Journal of Composites and Advanced Materials, 29 (4).

[21] Ouedraogo, M., Dao, K., Millogo, Y., Seynou, M., Aubert, J. E., & Gomina, M. (2017). Influence of kenaf (Hibiscus altissima) fibers on the physical and mechanical properties of adobes. Journal of the West African Chemical Society, 43, 48-63.

[22] Laibi, B. (2017). Hygro-thermo-mechanical behavior of structural materials for construction combining kenaf fibers with clay soils (Doctoral dissertation, Normandie).

[23] Osabor, V. N., Okafor, P. C., Ibe, K. A., & Ayi, A. A. (2009). Characterization of clays in Odukpani, south eastern Nigeria. African Journal of Pure and Applied Chemistry, 3 (5), 079-085.

[24] Mrklić, Ž. & Kovačić, T. (1998). Thermogravimetric investigation of volatility of dioctyl phthalate from plasticized poly (vinyl chloride). Thermochimica acta, 322 (2), 129-135. https://doi.org/10.1016/S0040-6031(98)00479-1

[25] Shanmugharaj, A. M., Bae, J. H., Lee, K. Y., Noh, W. H., Lee, S. H., & Ryu, S. H. (2007). Physical and chemical characteristics of multiwalled carbon nanotubes functionalized with aminosilane and its influence on the properties of natural rubber composites. Composites Science and technology, 67 (9), 1813-1822. https://doi.org/10.1016/j.compscitech.2006.10.021

[26] Benbayer, C. (2014). Nanocomposites based on clay and polymerizable surfactants (surfmers): synthesis and properties (Doctoral dissertation, Université Nice Sophia Antipolis). https://tel.archives-ouvertes.fr/tel-01142111

[27] Qtaitat, M. A., & Al-Trawneh, I. N. (2005). Characterization of kaolinite of the Baten El-Ghoul region/south Jordan by infrared spectroscopy. Spectrochimica Acta Part A: Molecular and Biomolecular Spectroscopy, 61 (7), 1519-1523. https://doi.org/10.1016/j.saa.2004.11.008

[28] Risite, H. (2015). Polymer/montmorillonite nanocomposites: Role of interactions generated by clay/polymer modification on morphology and structural, thermal, rheological and mechanical properties.

[29] Hongping, H., Ray, F. L., & Jianxi, Z. (2004). Infrared study of HDTMA+ intercalated montmorillonite. Spectrochimica Acta Part A: Molecular and Biomolecular Spectroscopy, 60 (12), 2853-2859. https://doi.org/10.1016/j.saa.2003.09.028

[30] Belver, C., Bañares Muñoz, M. A., & Vicente, M. A. (2002). Chemical activation of a kaolinite under acid and alkaline conditions. Chemistry of materials, 14 (5), 2033-2043. https://doi.org/10.1021/cm0111736